Magnetic state modification induced by superconducting response in ferromagnet/superconductor Nb/Co superlattices

C. Monton, F. de la Cruz, and J. Guimpel
Centro Atómico Bariloche, Instituto Balseiro, Comisión Nacional de Energía Atómica, Universidad Nacional de Cuyo, (8400) San Carlos de Bariloche, Argentina

(Received 14 August 2007; revised manuscript received 28 January 2008; published 19 March 2008)

Magnetization measurements in superconductor/ferromagnet Nb/Co superlattices show a complex behavior as a function of temperature, applied field, and sample history. Based on a simple model, it is shown that this behavior is due to an interplay between the superconductor magnetization temperature dependence, the ferromagnet magnetization time dependence, and the stray fields of both materials. It is also shown that the magnetic state of the Co layers is modified by the Nb superconducting response, implying that the problem of a superconductor/ferromagnetic heterogeneous sample has to be solved in a self-consistent manner.

DOI: 10.1103/PhysRevB.77.104521 PACS number(s): 74.78.Fk, 74.45.+c, 75.70.Cn

The interaction between a superconductor (SC) and a ferromagnet (FM) in close contact at an interface, as in a superlattice, has attracted attention in the last years due to the possibility of fabricating SC/FM hybrid devices.[1] These engineered materials originate the appearance of interesting physical phenomena due to the different mechanisms of interaction, such as SC pair breaking effects related to exchange interaction at the interface,[1] or electromagnetic interaction with the stray fields of the FM both at the mesoscopic and macroscopic levels.[2–4]

Some recent publication shows the ways in which the FM affects the SC response. For example, in the domain wall superconductivity effect,[2–4] superconductivity nucleates on domain walls where stray fields are close to zero. Another interesting phenomenon is the spin switch effect used to explain the superconducting response of FM/SC/FM trilayers[1,5,6] where the FM layers are either ferro- or antiferromagnetically oriented. However, some recent publications suggest that the stray fields of the FM layers should be considered to explain the superconducting response of similar configurations.[7] The relevance of the stray field in superlattices has been recently demonstrated by us[8] where the superposition of the applied and stray fields quantitatively explains the magnetic response of Nb/Co superlattices.

In contrast, very little work has been done in exploring the way in which the SC affects the magnetic state of the FM layer, as theoretically suggested in Ref. 9 Dubonos *et al.*[10] have reported magnetization studies of FM/SC structures of submicron size. They demonstrate that the stray fields around a ferromagnet on top of a SC material are distorted by the superconducting shielding currents below the superconducting transition temperature T_{CS}. In Ref. 8, we suggested the possibility that the SC response may modify the magnetic state of the FM layers. A recent work by Wu *et al.*[11] shows, for a $[Nb/Ni_{81}Fe_{19}/Nb/Ni_{81}Fe_{19}/Nb]$ heterostructure, that FM layer's magnetization is reduced after the sample is cooled below T_{CS}. The experiment was performed with the FM layers in the remnant state (i.e., zero applied field). They also observe that the superconducting response is ferromagnetically oriented with the FM layer's magnetization as previously found in FM/antiferromagnet/SC systems.[12]

In the present work, we explore the FM layer's magnetization changes induced by the superconducting transition for different magnetic initial states of the FM layers. We observe that, indeed, the SC response modifies the magnetic state of the FM layers, and we understand and model the global electromagnetic response as determined by an interplay between the SC magnetization temperature dependence and the FM magnetization time evolution.

We present data on the temperature T dependence of the magnetic flux expulsion $\Delta\phi$ directly proportional to the SC magnetization for Nb/Co superlattices. Data are presented for $[Nb(44\ nm)/Co(10\ nm)]\times 19$ and $[Nb(44\ nm)/Co(7.5\ nm)]\times 19$ superlattices. The results on these samples are representative of the measurements we performed on a collection of Nb/Co FM/SC superlattices. Since our experimental setup measures magnetic flux variations,[8] all $\Delta\phi$ values are measured with respect to the first data point, always above the superconducting critical temperature T_{CS}. Sample preparation, characterization method, and measurement details are described in Ref. 8. For all flux expulsion data, the applied field H_a is parallel to the sample surface. In the normal state, both superlattices present FM behavior with Curie temperatures T_C of above 300 K. Flux expulsion in the SC state was measured as a function of T in field cooling experiments for two different Co layer's initial FM states; −FC, with the Co layers initially saturated in the negative H_a direction, and +FC, with the Co layers initially saturated in the positive H_a direction. A detailed explanation of these measurement protocols is also included in Ref. 8.

Figure 1 is a composite that summarizes the experimental results. In the main panel, we show the FM hysteresis loop of the Co layers at $T=7$ K, close but above T_{CS} of the Nb layers. In the superimposed panels, we show the T dependence of $\Delta\phi$ for +FC and −FC measurements. For each initial state, several T cycles were measured, each cycle sweeping T down from 7 to 5.5 K and up to 7 K again. The solid dots in the hysteresis curve connected with arrows to the panels indicate the initial magnetic state for each experiment.

The data for the first T down sweep in each panel show the behavior already discussed in our previous work.[8] As discussed there, the SC response is proportional to the effective field H_{eff}, originated by the superposition of the applied

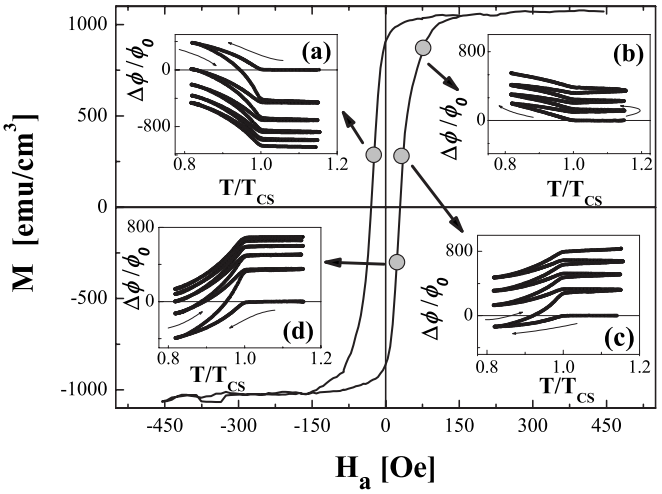

FIG. 1. Main panel: magnetization M as a function of applied field H_a for the $[\mathrm{Nb}(44\ \mathrm{nm})/\mathrm{Co}(10\ \mathrm{nm})]\times 19$ superlattice at $T=7\ \mathrm{K} > T_{CS}=6.2\ \mathrm{K}$. Panels (a)–(d) show the temperature T dependence of the superconducting magnetic flux response $\Delta\phi$ in units of the superconducting flux quantum ϕ_0 at different applied fields and ferromagnetic layer initial states, as indicated by gray dots and connecting arrows in the main panel. Arrows in panels indicate the direction of the T sweeps. Panel (a): $H_a=-22$ Oe, +FC. Panel (b): $H_a=75$ Oe, −FC. Panel (c): $H_a=38$ Oe, −FC. Panel (d): $H_a=22$ Oe, −FC.

field H_a and the Co layers' stray field H_s. For the −FC measurements (lower branch of the Co hysteresis loop), at low H_a and negative Co magnetization, the SC layers sense a positive H_{eff} due to the Co H_s [see panel (d)]. At higher H_a, the Co magnetization becomes positive, H_s becomes negative and larger than H_a, and the SC senses a negative H_{eff} [see panel (b)]. Panel (c) shows an intermediate case, where the magnetization is already reversed, but H_s is smaller than H_a and the SC still senses a positive H_{eff}. Panel (a), +FC initial state (upper branch of the Co hysteresis loop) is the mirror experiment from panel (d).

The feature observed in these data is present in the dependence of the Co magnetization in the normal state with the number of T sweeps, i.e., cycles. This dependence is observed as a nonrepeatability of the normal state magnetization value after a cycle is completed. This behavior is not due to an experimental artifact related to an instrumental drift, since this instrumental drift has been substracted from the data. A systematic behavior is observed in spite of the seemingly complex dependence. The direction of the variation follows the sign of the *applied* field, and it is independent of the Co magnetization direction, i.e., the *stray* field, compare the data in panels (b) and (d), for example. The difference between the first and second normal state $\Delta\phi$ values in panel (d) of 360 superconducting flux quantums is equivalent to a change of 1.1 emu cm^{-3} in the Co layer's magnetization, which shows that this effect is small but not negligible.

In order to understand this behavior, we constructed a simple "toy model" to qualitatively simulate the experimental data. Although the model is very simple, a careful consideration of its hypothesis should be made to fully understand the implications of the results.

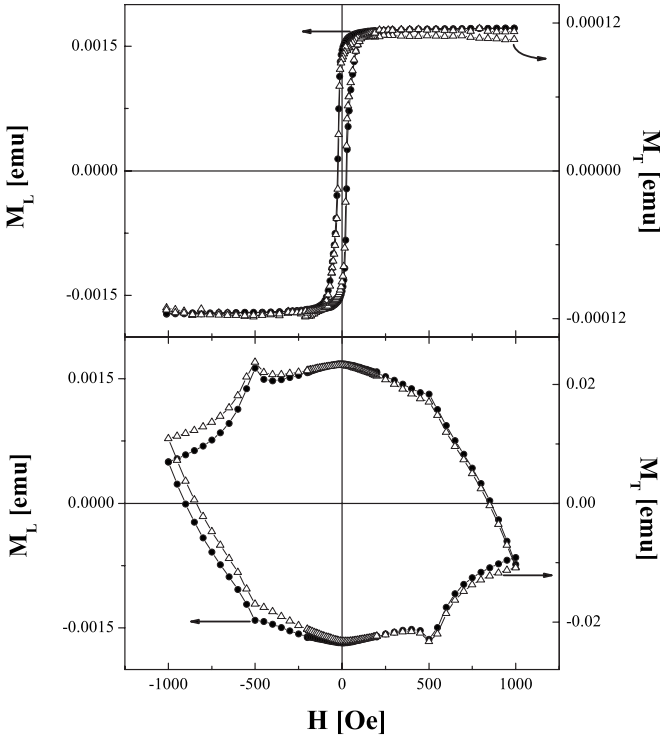

FIG. 2. Hysteresis loop for the superlattices $[\mathrm{Nb}(44\ \mathrm{nm})/\mathrm{Co}(10\ \mathrm{nm})]\times 19$ at $T=7$ K, normal state (upper panel), and $[\mathrm{Nb}(44\ \mathrm{nm})/\mathrm{Co}(0.7\ \mathrm{nm})]\times 7$ at $T=3$ K, superconducting state (lower panel). Arrows show the corresponding scale for the longitudinal (black circles) and transverse (open triangles) signals. The $t_{\mathrm{Co}}=0.7$ nm sample is not ferromagnetic.

We have previously shown[8] that proximity effects are present in our system due to the absence of insulator layers between SC and FM layers. Since our model tries to explain the macroscopic electrodynamic response, only electrodynamic interactions will be considered. Any work regarding the particular value of the critical temperature or the SC gap should include the proximity effects as their main ingredient.

In Ref. 13, it was observed that a transverse magnetization develops in NiFe/Nb/NiFe trilayers near the coercive field at the normal state. In Ref. 11, it was proposed that the FM magnetization changes are related to the out-of-plane magnetization induced by the SC response. In order to verify if this out-of-plane FM magnetization state is present in our samples, we measured the longitudinal and transverse hysteresis loops with applied field parallel to the sample's surface, above T_{CS}, for a $[\mathrm{Nb}(44\ \mathrm{nm})/\mathrm{Co}(10\ \mathrm{nm})]\times 19$ superlattice (see upper panel of Fig. 2).

Although a transverse magnetization is measured, it is clear that it scales perfectly with the longitudinal one in the normal state, $T=7$ K. This indicates that the transverse signal is not due to an intrinsic transverse magnetization but to a misalignment angle α of about 4° between the sample and the applied field, best alignment that we can obtain without a specially designed sample holder for the commercial superconducting quantum interference device magnetometer. As a second cross-check, if a similar misalignment is present in a pure SC sample, it is expected for the transversal signal to be larger than the longitudinal one, since the SC Meissner

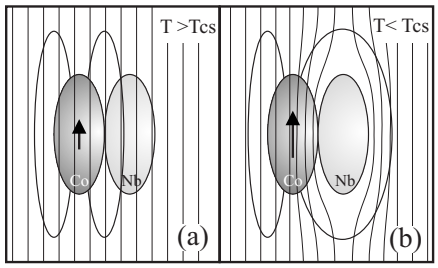

FIG. 3. Schematics of the toy model behavior. Panel (a): at $T > T_{CS}$, the normal Nb ellipsoid experiences an effective field due to the applied field (straight lines) and the ferromagnetic Co ellipsoid stray field (dipolelike lines). Panel (b): as T is reduced below T_{CS}, the magnetic flux expulsion from the Nb ellipsoid modifies the effective field over the Co ellipsoid.

magnetization is proportional to the sample area and the transversal area is several orders of magnitude larger than the longitudinal one. The lower panel of Fig. 2 shows the longitudinal and transverse signals for a $[\mathrm{Nb}(44\ \mathrm{nm})/\mathrm{Co}(0.7\ \mathrm{nm})]\times 7$ superlattice at $T=3\ \mathrm{K} < T_{CS}$, sample which does not show FM behavior. The transversal signal is clearly larger than the longitudinal one, even for the sample aligned almost parallel to the applied field. The misalignment angle is again about 4° between the sample and the applied field. From these results, it is evident that our samples do not present out-of-plane magnetization. We also performed magnetic force microscopy measurements with applied field normal to the sample, which did not show out-of-plane magnetization rotation for applied fields of up to 1 T. This difference between the Nb/NiFe bilayers,[13] Nb/NiFe pentalayers,[11] and our Nb/Co multilayers could be due to a number of factors such as the different FM materials (Co vs NiFe), presenting different intrinsic anisotropies, or the different layer's thicknesses with probably different roughnesses. A direct comparison for all the mentioned factors was difficult between the studied systems. In conclusion, our Co layers present only in-plane magnetization, and no intrinsic transverse magnetization is considered in the model.

Having taken into account the above conditions, the first requirement for the model is that an electromagnetic stray-field mediated interaction should exist between the FM and the SC components. This is not achievable if the materials are modeled as nearly infinite slabs parallel to the applied field, since the stray field of this geometry is negligible. Using simulations, Steiner and Ziemann[7] have demonstrated that the domain structure of thin FM layers originates a non-negligible perpendicular stray field. Using this ideas, we modeled both materials as ellipsoids with one of the principal axes parallel to the field. The toy model sample consists, then, of FM and SC ellipsoids, located side by side. Figure 3 depicts the main ideas of the model. Panel (a) shows the situation at $T > T_{CS}$ where the H_{eff} sensed by the SC ellipsoid is composed by H_a (straight lines) and the FM H_s (dipolar lines arising from the FM ellipsoid). When T is reduced below T_{CS}, as depicted in panel (b), the flux expulsion from the SC ellipsoid modifies the H_{eff} sensed by the FM ellipsoid and consequently its magnetization. The solution of the problem has now to be found in a self-consistent way.

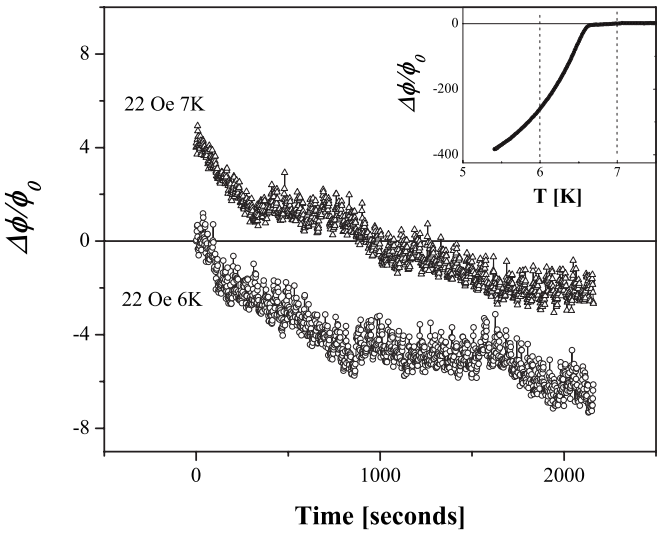

FIG. 4. Time t dependence of the sample magnetization change $\Delta\phi$ at $T > T_{CS}$ (triangles) and $T < T_{CS}$ (circles) for 22 Oe−FC magnetic initial state. The inset shows the temperature dependence of the sample magnetization change $\Delta\phi$. Dashed lines in the inset show the temperatures at which drifts were measured.

The ellipsoid shape or eccentricity ϵ was selected as to maximize the stray-field effects. That an optimum value exists is clear from the fact that in the $\epsilon \to \infty$ "needle" limit, the stray fields approach zero due to the negligible demagnetizing effects, and that in the $\epsilon \to 0$ "disk" limit, the stray fields also approach zero since the ellipsoid is being magnetized along the shape anisotropy "hard axis." The optimal ϵ value actually depends on the material's magnetization, but since it is weakly dependent on it, a value of 10 was found to maximize the stray-field effects in nearly all the T-H_a range. Also, since an exact three dimensional spatial solution of this electromagnetic problem is beyond the scope of this work, and would only obscure the results of the model, the spatial dependence of the stray fields is neglected, and H_s due to each ellipsoid is evaluated only at the center of the other ellipsoid.

The second ingredient in the model is a "time" dependence. This dependence cannot be ascribed to the superconducting material since we have shown that no vortices are present in the T-H_a range of these experiments.[8] Therefore, it must be arising from the creep in the FM material. In order to verify this idea, we measured the magnetization time dependence just above and just below T_{CS} for a given initial magnetic state of the FM layers. The results are shown in Fig. 4 where it is clear that the SC state has no effect on the time dependence. Consequently, the magnetization of the SC Nb ellipsoid is modeled by a T dependent, time independent Meissner state. As a further simplification of the model, the T dependence is forced to follow that of a parallel slab with a two fluid T law. On the other hand, the FM Co ellipsoid magnetization does not present a T dependence since its T_C is much higher than the measurement range. It only shows a time dependence which must be numerically simulated, as described in the next paragraph.

To simulate the T sweeps at constant H_a, the self-consistent equilibrium state of the magnetized ellipsoids is solved at a given T. After this, the magnetization change for

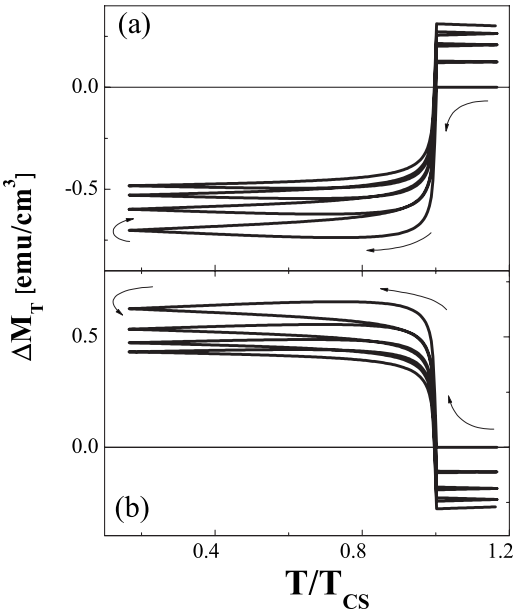

FIG. 5. Model prediction for the temperature T dependence of the sample magnetization change, $\Delta M_T = M_T(T) - M_0$, where M_0 is the magnetization for the initial simulated data point at $T > T_{CS}$. Panels (a) and (b) show the results for two sets of parameters qualitatively equivalent to the experimental data in panels (c) and (a) of Fig. 1. Panel (a): $H_a = 22.85$ Oe, $M_0 = 5.12$ emu cm^{-3}. Panel (b): $H_a = -17.15$ Oe, $M_0 = 5.12$ emu cm^{-3}.

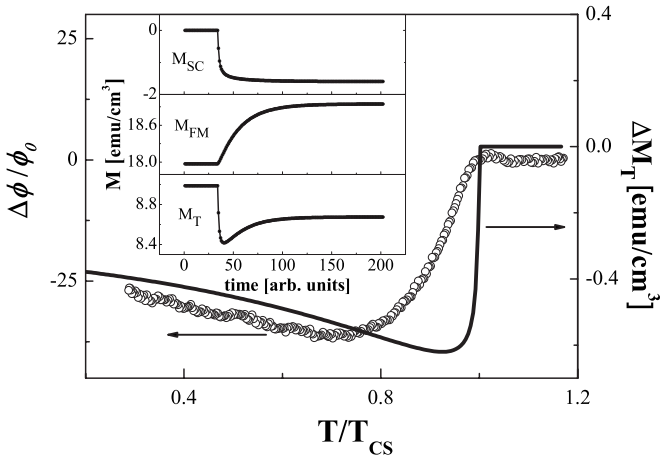

FIG. 6. Magnetic flux expulsion, $\Delta\phi$, for a [Nb(44 nm)/Co(7.5 nm)]×19 superlattice with $T_{CS} = 5.9$ K, and model prediction, ΔM_T, for $H_a = 15$ Oe and $M_0 = 9$ emu cm^{-3}. The inset shows the dependence on simulated data point number, i.e., time, for the superconducting ellipsoid magnetization M_{SC}, the ferromagnetic ellipsoid magnetization M_{FM}, and the sample's total magnetization, M_T.

the Co ellipsoid is reduced by a given percentage, and the magnetization of the Nb ellipsoid is recalculated for this, now fixed, value of the Co ellipsoid's magnetization, i.e., stray field. This algorithm results in an effective exponential time dependence for the Co magnetization. The sample's magnetization M_T is defined as the total magnetic moment divided by the total sample volume. In order to compare the results to the experiments, the simulation data are presented as $\Delta M_T = M_T - M_0$, where M_0 is the value for the first simulated point, always at $T > T_{CS}$.

Panels (a) and (b) in Fig. 5 show the prediction of the model for situations similar to panels (c) and (a) in Fig. 1, i.e., opposite direction of H_a and same value of M_0. It is clear that the principal features of the experimental data are qualitatively reproduced. First, there is a dependence of the normal state magnetization with the number of cycles. This dependence follows the sign of the applied field and is not correlated to the magnetization direction. Second, there is an irreversibility between cooling-down and warming-up sweeps. Third, a nonmonotonic T dependence is observed for cooling-down sweeps.

An interesting feature not actually observable in the data in Fig. 1, but presented in Ref. 8, is the nonmonotonic T dependence that develops for applied fields near the coercive field of the Co layers (see Fig. 6). The main panel in Fig. 6 shows a comparison between experimental and simulated data, where the simulation parameters have been selected as to maximize this nonmonotonic T dependence. The origin of this behavior becomes clear when examining separately the Nb and Co magnetization responses in the simulated data. Since it will be evident that the time dependence of the Co layers plays a key role in the explanation of this effect, the inset shows the SC ellipsoid magnetization M_{SC}, the FM ellipsoid magnetization M_{FM}, and the sample's magnetization M_T as a function of simulated data point number, i.e., time, while T is swept down from above T_{CS}. The T sweep is linear with this "simulated time." The time dependence of M_{SC} is that arising from the T sweep, given that the Meissner state does not present an intrinsic time dependence. The time dependence of M_{FM}, on the other hand, has a twofold origin. First, the flux expulsion in the SC originates an increase of local magnetic field in the FM material, as schematized in panel (b) of Fig. 3. Second, the M_{FM} presents an intrinsic time dependence in its response to the magnetic field changes. In this light, the origin of the nonmonotonic T dependence becomes clear. As T is swept down from above T_{CS}, the T dependence of the SC ellipsoid magnetization produces a flux expulsion, which originates a field increase in the FM material, increasing its M_{FM}. At lower temperatures (simulated time longer than 45 in the inset), the T dependence of the SC material is relatively weak, while the FM material is still changing as a function of time, and this time dependence of the FM material originates a seemingly "nonmonotonic" signal.

The results and the toy model presented here clarify the response of SC/FM hybrid structures and, at the same time, raise an interesting question. We have demonstrated that the electrodynamic response of these hybrid systems involves a combination of two separate phenomena. In the first place, the diamagnetic response of the SC layers expels the magnetic flux into the FM layers. As a consequence, the FM material responds with a time dependence, clearly in the direction of the applied field. Both materials affect each other with their respective stray fields. In this process, the magnetic domain structure of the FM seems to play an important role, since the stray fields of an infinite slab are negligible.

Clearly, in order to observe stray-field effects, a nonslab geometry inspired in a real ferromagnetic domain distribution[7] has to be present in the samples. In this picture, an interesting point arises. Given that the response of the hybrid material is affected, and in some T and H range, dominated, by the intrinsic time dependence, the effects described here may be important if the device operation is based on magnetization *changes* and designed to work at frequencies similar to the creep of the FM.

In summary, we have demonstrated that the electrodynamic response of SC/FM hybrid materials is determined by an interplay between the temperature dependence of the SC magnetization, the time dependence of the FM magnetization, and the effective interaction between them mediated by the stray fields.

Work partially supported by ANPCyT PICT2003-03-13511, ANPCyT PICT2003-03-13297, and Fundación Antorchas. C.M. acknowledges financial support from CONICET, Argentina.

[1] J. Y. Gu, C.-Y. You, J. S. Jiang, J. Pearson, Ya. B. Bazaliy, and S. D. Bader, Phys. Rev. Lett. **89**, 267001 (2002).
[2] A. Yu. Rusanov, M. Hesselberth, J. Aarts, and A. I. Buzdin, Phys. Rev. Lett. **93**, 057002 (2004); Z. Yang, M. Lange, A. Volodin, R. Szymczak, and V. V. Moshchalkov, Nat. Mater. **3**, 793 (2004).
[3] D. Stamopoulos and M. Pissas, Phys. Rev. B **73**, 132502 (2006).
[4] W. Gillijns, A. Yu. Aladyshkin, M. Lange, M. J. Van Bael, and V. V. Moshchalkov, Phys. Rev. Lett. **95**, 227003 (2005).
[5] Ion C. Moraru, W. P. Pratt, Jr., and Norman O. Birge, Phys. Rev. B **74**, 220507(R) (2006).
[6] A. Yu. Rusanov, S. Habraken, and J. Aarts, Phys. Rev. B **73**, 060505(R) (2006); A. Singh, C. Sürgers, and H. v. Löhneysen, *ibid.* **75**, 024513 (2007).
[7] R. Steiner and P. Ziemann, Phys. Rev. B **74**, 094504 (2006).
[8] C. Monton, F. de la Cruz, and J. Guimpel, Phys. Rev. B **75**, 064508 (2007).
[9] L. N. Bulaevskii and E. M. Chudnovsky, Phys. Rev. B **63**, 012502 (2000).
[10] S. V. Dubonos, A. K. Geim, K. S. Novoselov, and I. V. Grigorieva, Phys. Rev. B **65**, 220513(R) (2002).
[11] Hong-ye Wu, Jing Ni, Jiang-wang Cai, Zhao-hua Cheng, and Young Sun, Phys. Rev. B **76**, 024416 (2007).
[12] D. Stamopoulos, N. Moutis, M. Pissas, and D. Niarchos, Phys. Rev. B **72**, 212514 (2005).
[13] D. Stamopoulos, E. Manios, and M. Pissas, Phys. Rev. B **75**, 184504 (2007).